

Reactions of Dihaloboranes with Electron-Rich 1,4-Bis(trimethylsilyl)- 1,4-diaza-2,5-cyclohexadienes

Li Ma[†], Xiaolin Zhang[†], Wenbo Ming[†], Shengxin Su, Xiaoyong Chang, Qing Ye*

Department of Chemistry, Southern University of Science and Technology, 518055
Shenzhen, P. R. China

* Correspondence: yeq3@sustech.edu.cn; Tel.: +86 (0)755-88018354

[†] These authors contributed equally to this work

Table of Contents

I. NMR Spectra of Products	2
II. Crystallographic details.....	20

I. NMR Spectra of Products

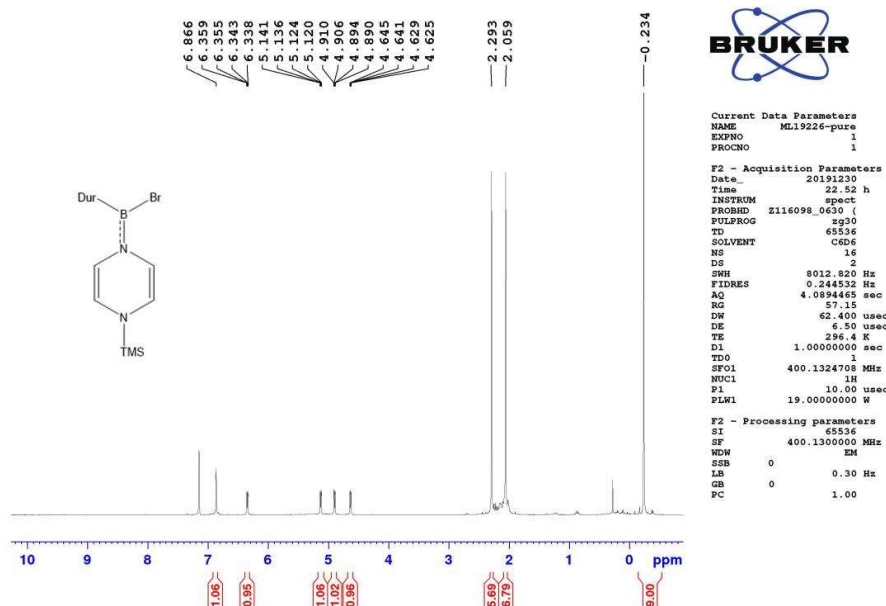


Figure S1. ¹H NMR (400 MHz, C₆D₆) of 3

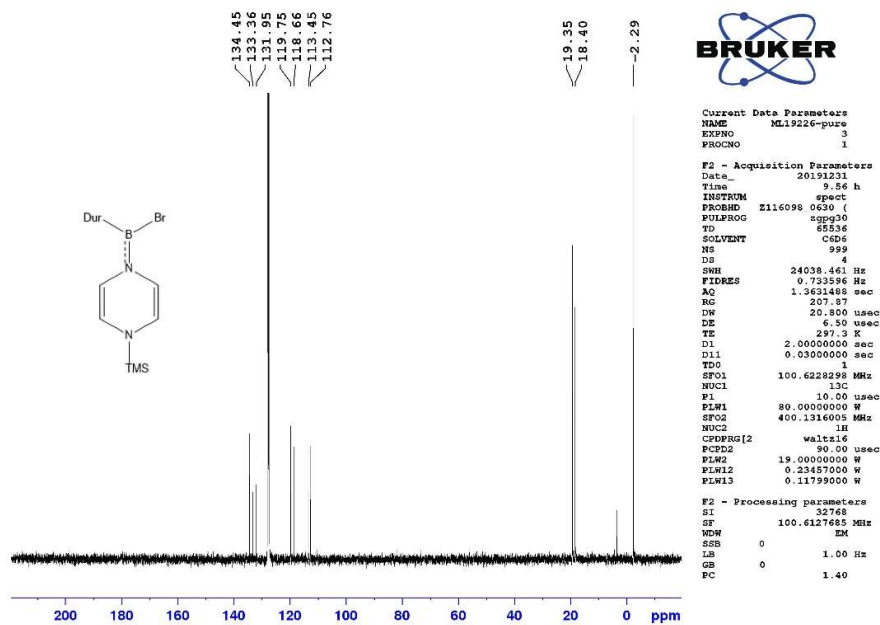


Figure S2. ¹³C{¹H} NMR (101 MHz, C₆D₆) of 3

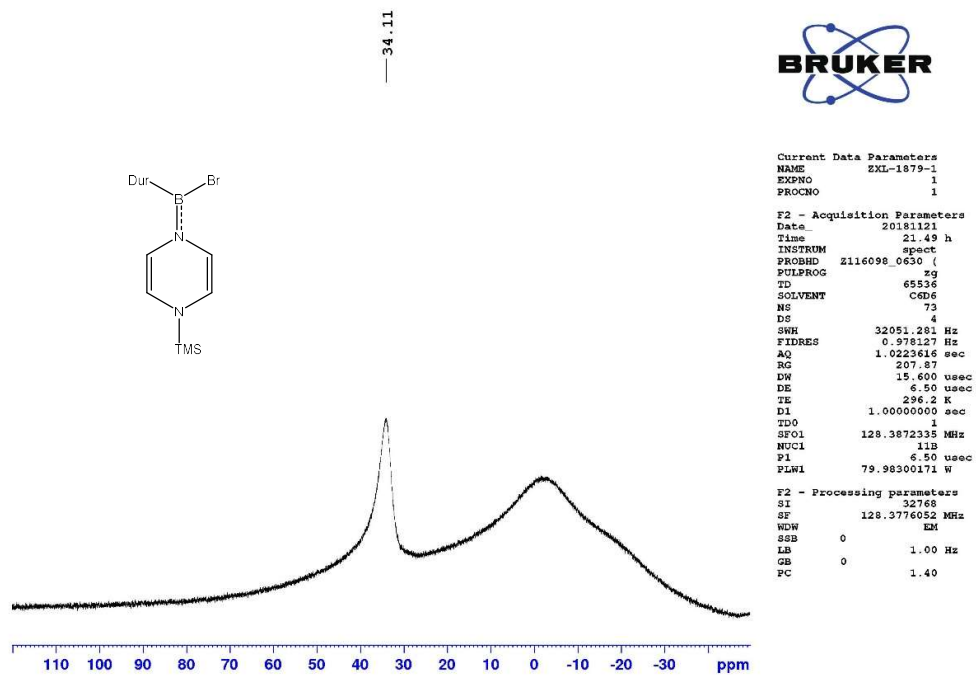


Figure S3. ^{11}B NMR (128 MHz, C_6D_6) of **3**

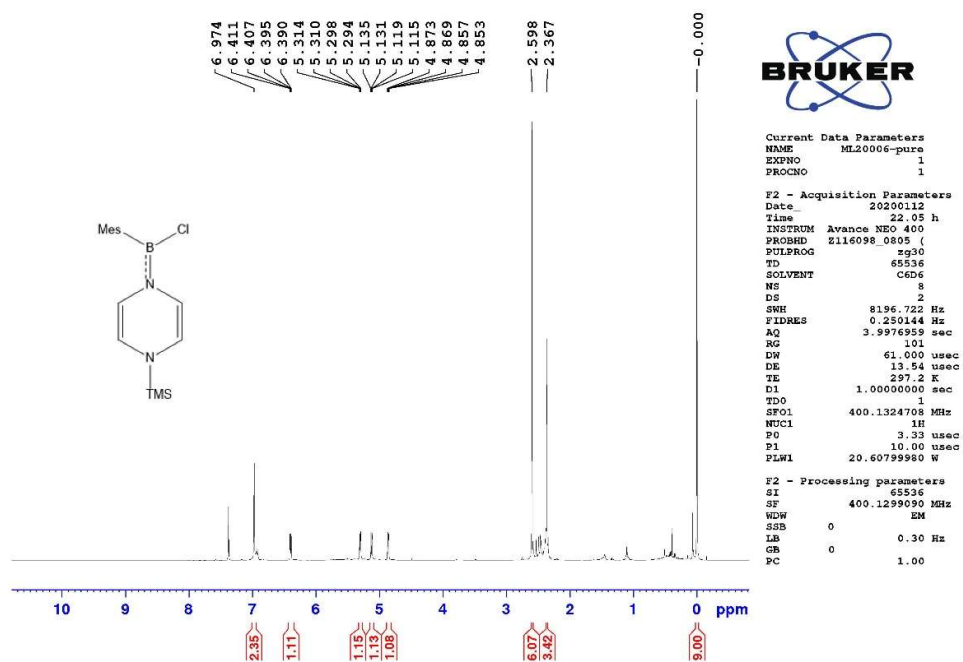


Figure S4. ^1H NMR (400 MHz, C_6D_6) of **4**

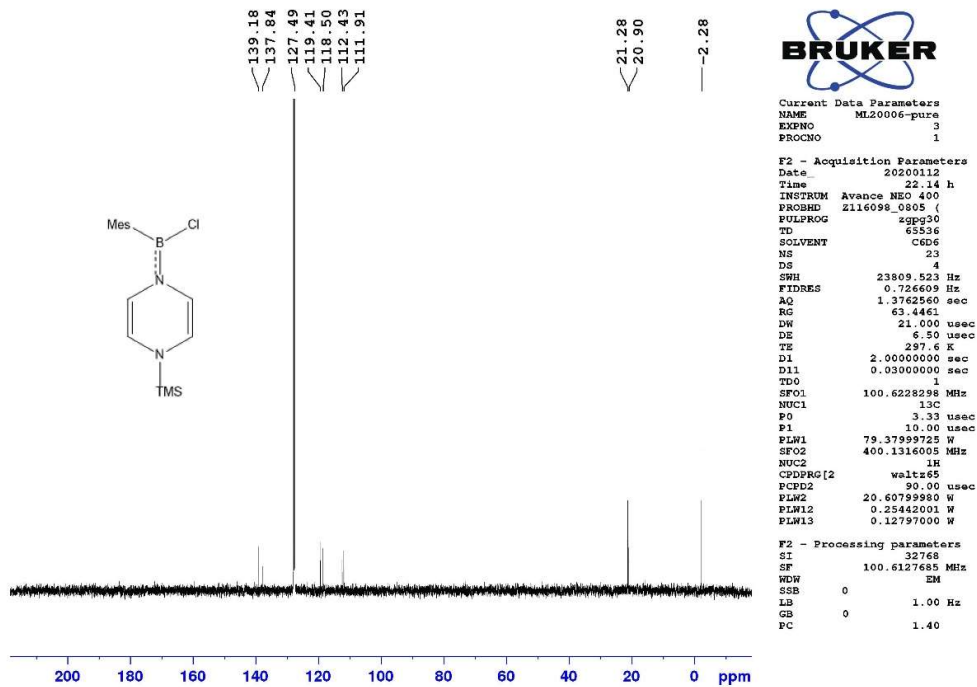


Figure S5. ¹³C{¹H} NMR (101 MHz, C₆D₆) of 4

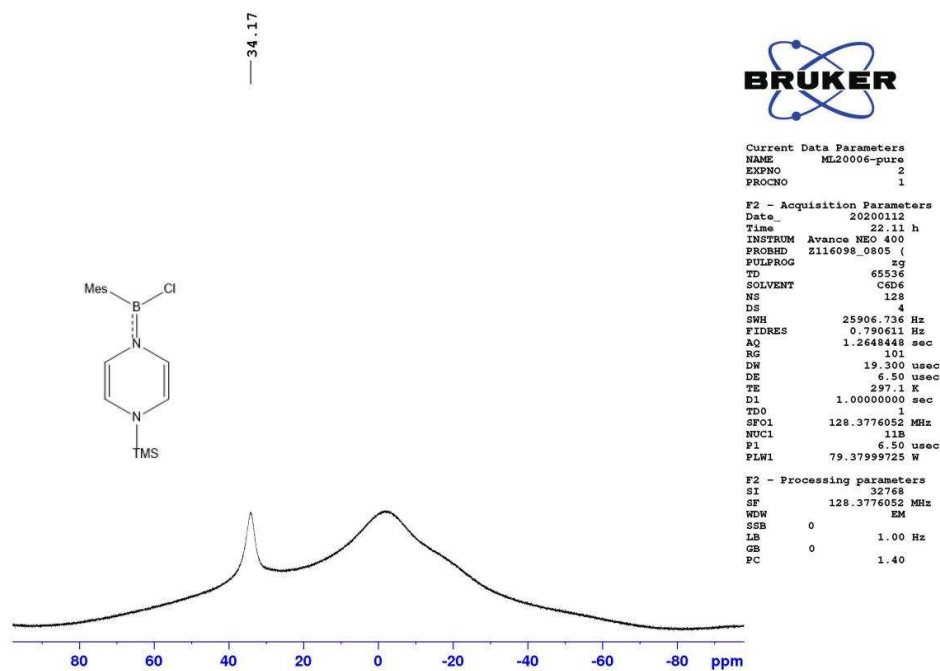


Figure S6. ¹¹B NMR (128 MHz, C₆D₆) of 4

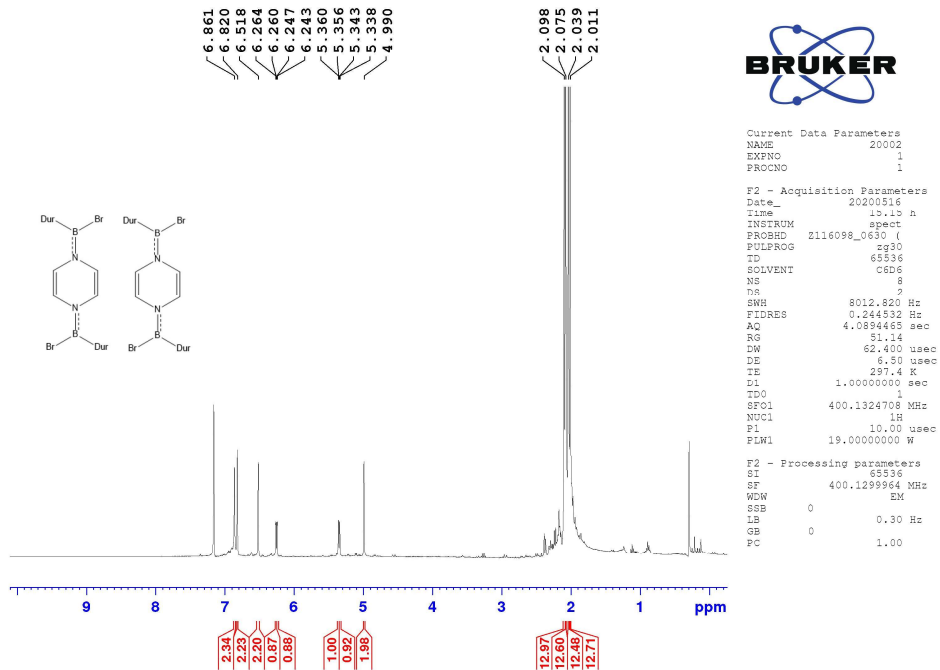


Figure S7. ^1H NMR (400 MHz, C_6D_6) of 5a + 5b

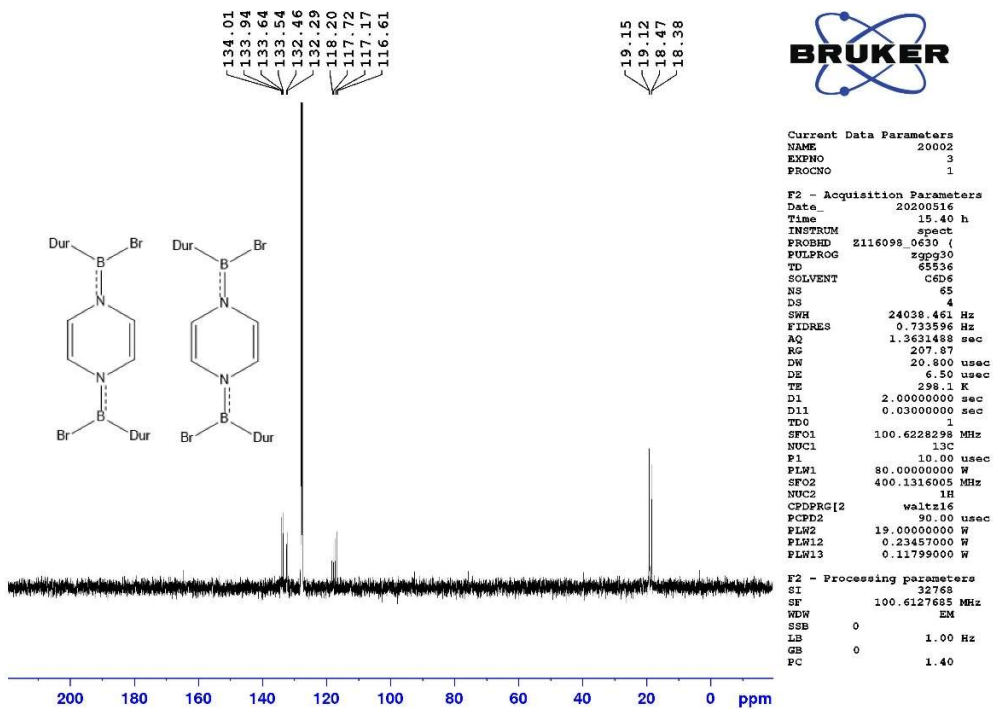


Figure S8. $^{13}\text{C}\{^1\text{H}\}$ NMR (101 MHz, C_6D_6) of 5a + 5b

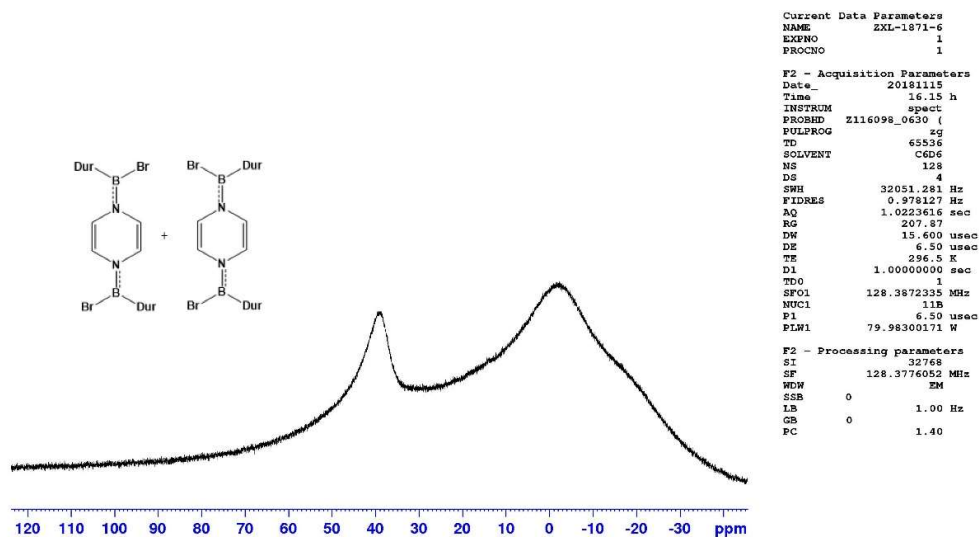


Figure S9. ¹¹B NMR (128 MHz, C₆D₆) of 5a + 5b

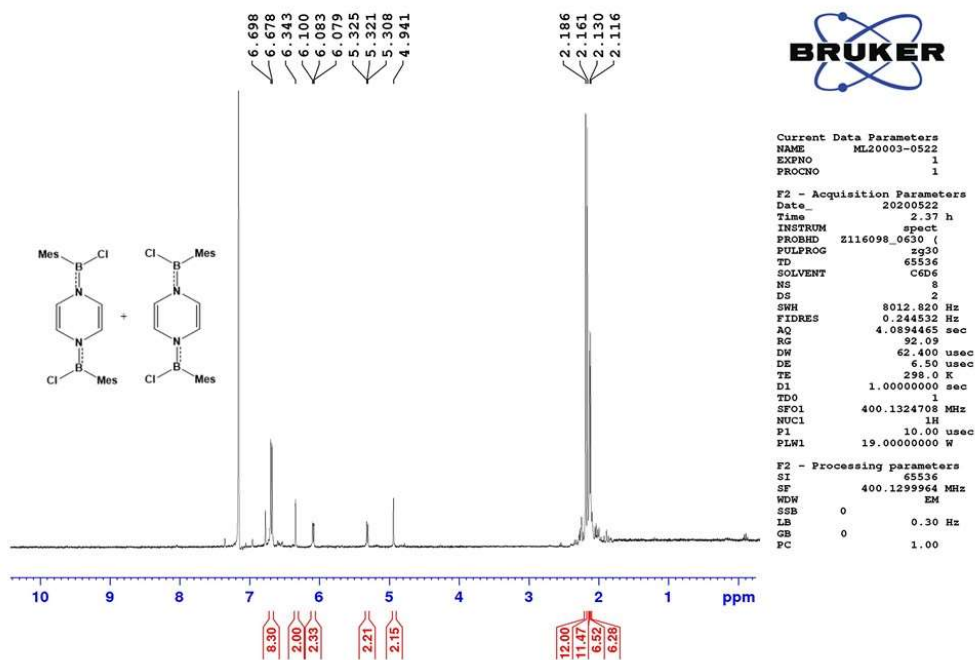


Figure S10. ¹H NMR (400 MHz, C₆D₆) of 6a + 6b

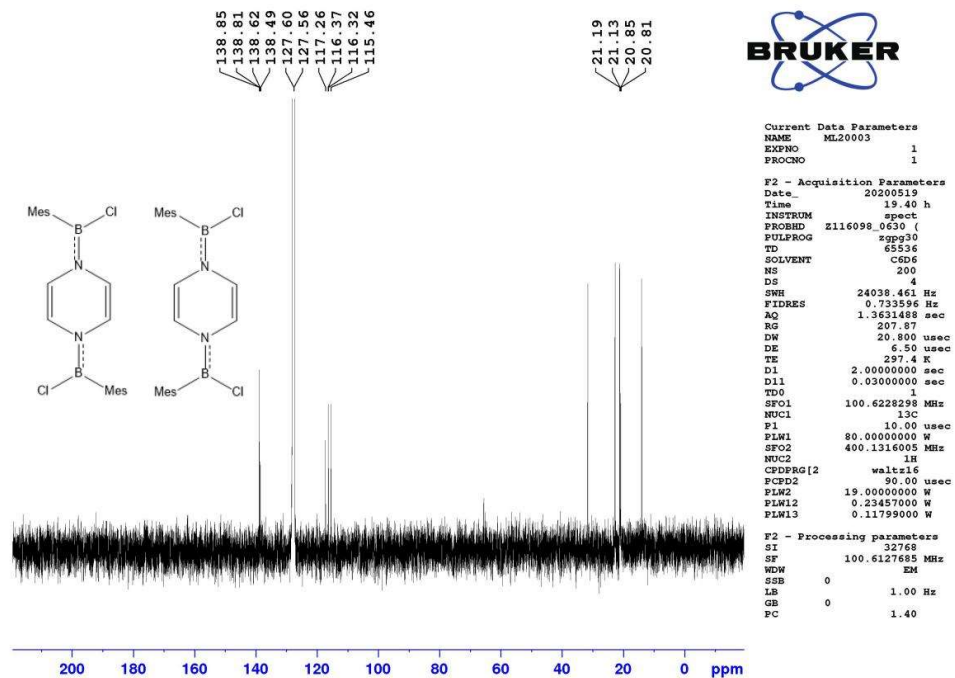


Figure S11. $^{13}\text{C}\{^1\text{H}\}$ NMR (101 MHz, C_6D_6) of **6a** + **6b**

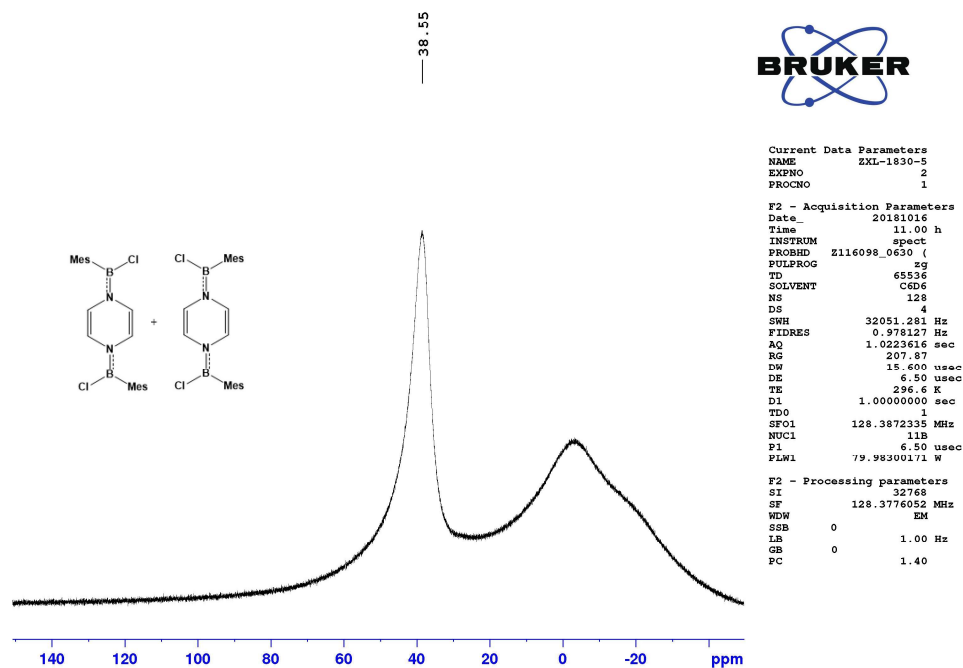


Figure S12. ^{11}B NMR (128 MHz, C_6D_6) of **6a** + **6b**

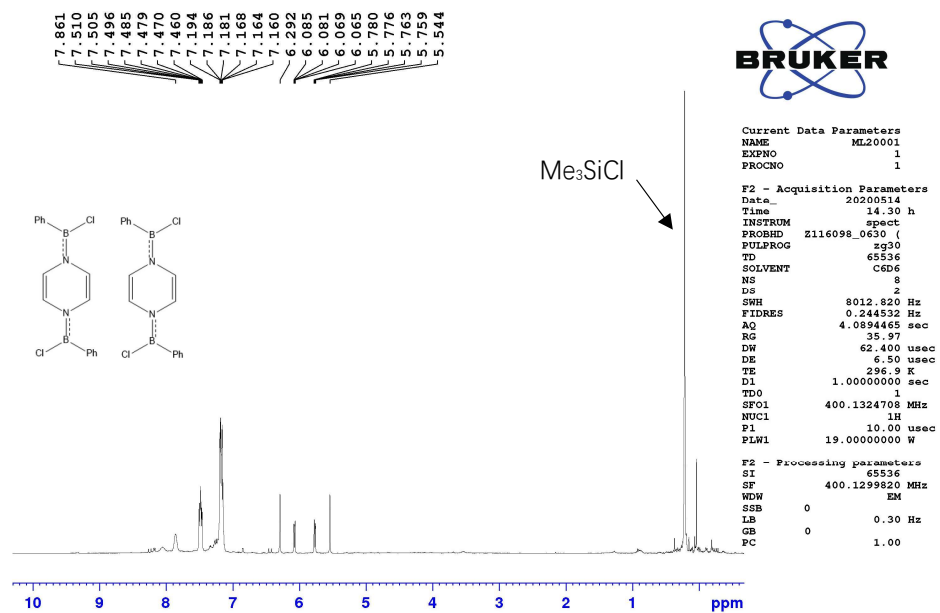


Figure S13. ^1H NMR (400 MHz, C_6D_6) of **7a** + **7b** (Complete removal of Me_3SiCl led to partial decomposition of **7a** and **7b**)

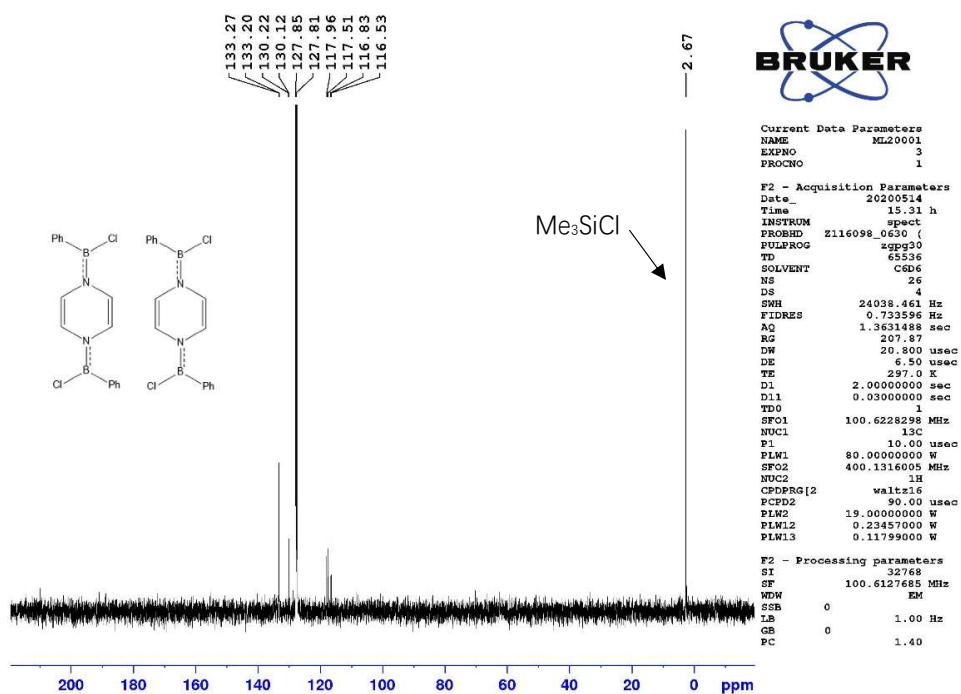


Figure S14. $^{13}\text{C}\{^1\text{H}\}$ NMR (101 MHz, C_6D_6) of **7a** + **7b** (Complete removal of Me_3SiCl led to partial decomposition of **7a** and **7b**)

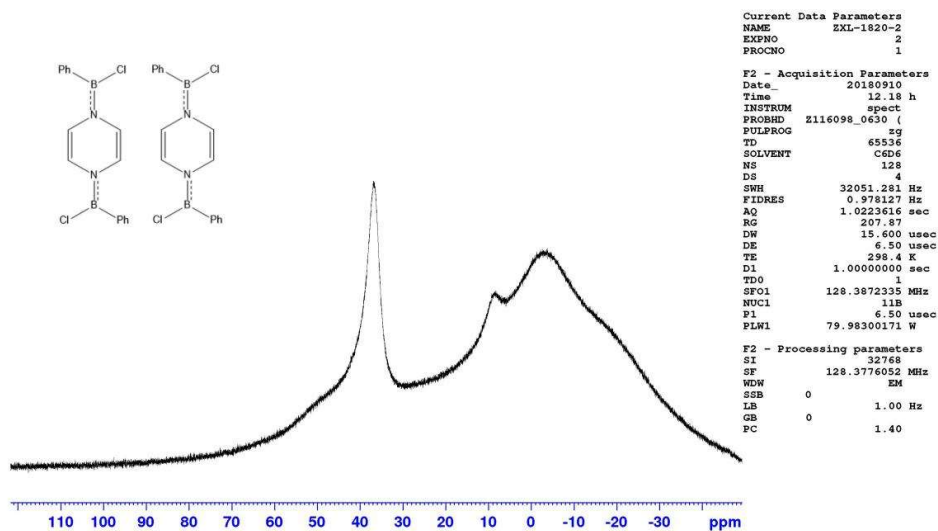


Figure S15. ¹¹B NMR (128 MHz, C₆D₆) of 7a + 7b

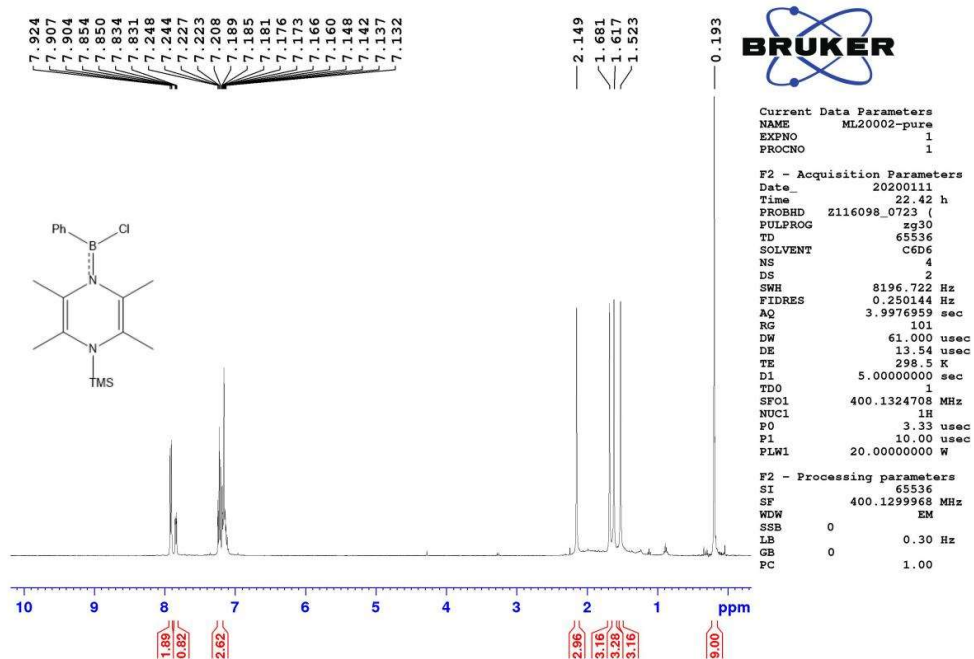


Figure S16. ¹H NMR (400 MHz, C₆D₆) of 8

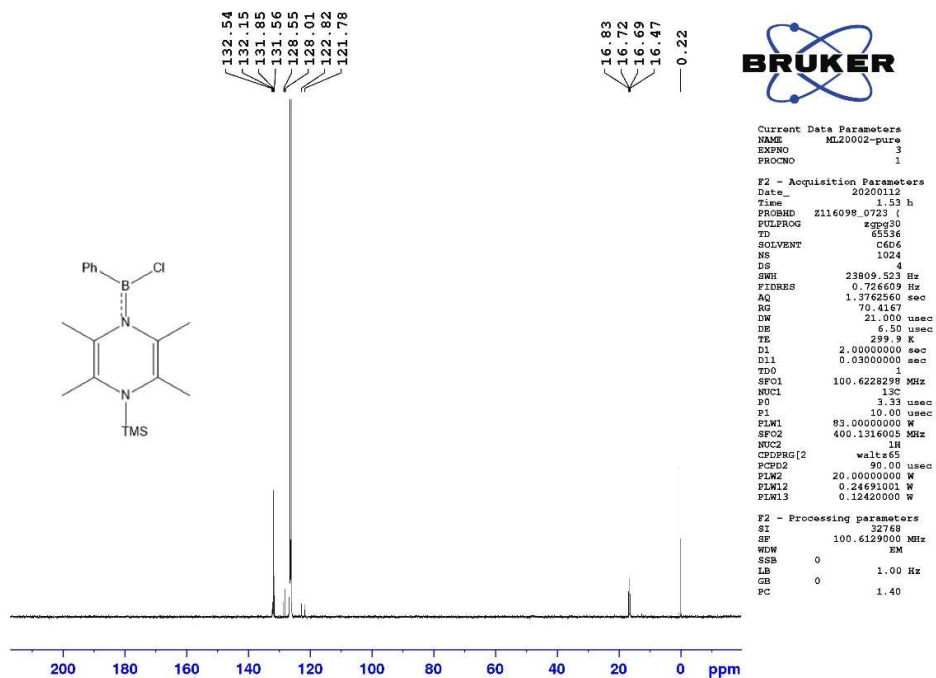


Figure S17. $^{13}\text{C}\{^1\text{H}\}$ NMR (101 MHz, C_6D_6) of **8**

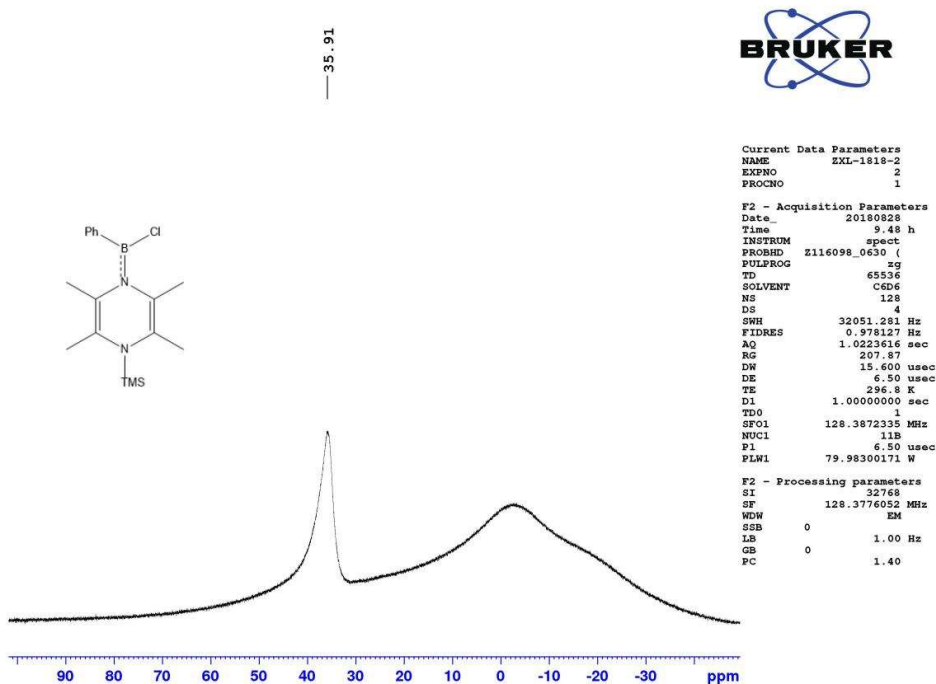


Figure S18. ^{11}B NMR (128 MHz, C_6D_6) of **8**

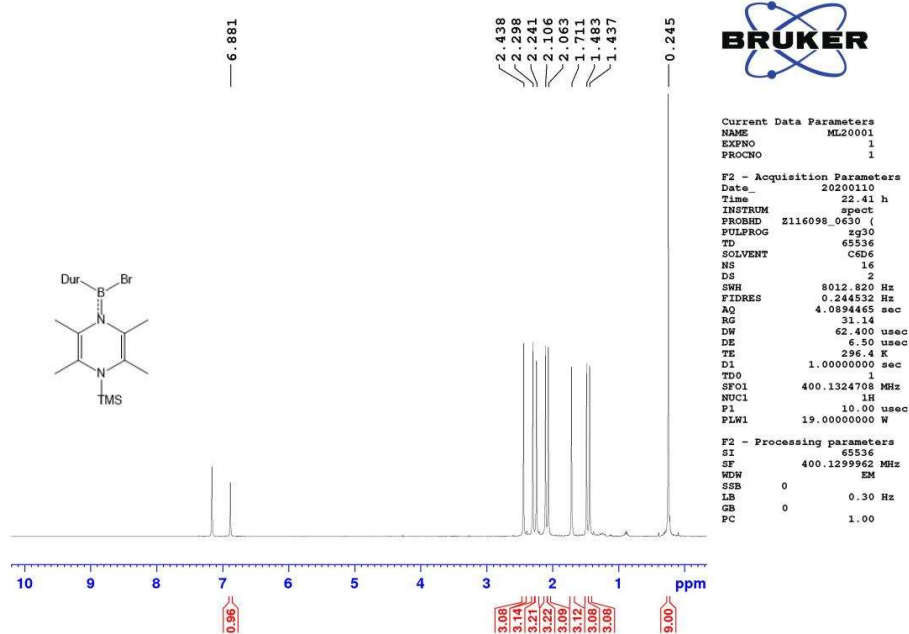


Figure S19. ^1H NMR (400 MHz, C_6D_6) of 9

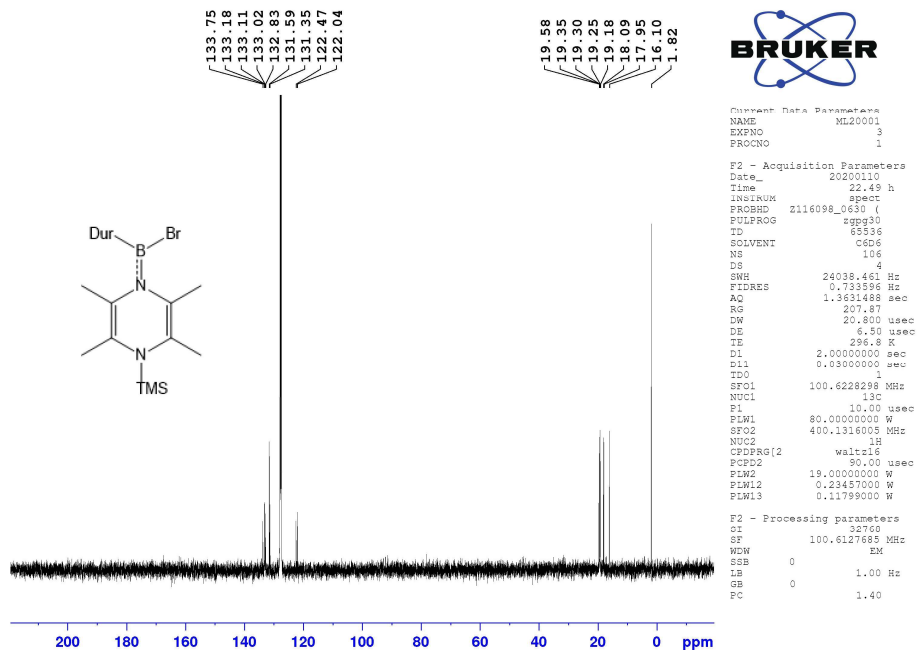


Figure S20. $^{13}\text{C}\{^1\text{H}\}$ NMR (101 MHz, C_6D_6) of 9

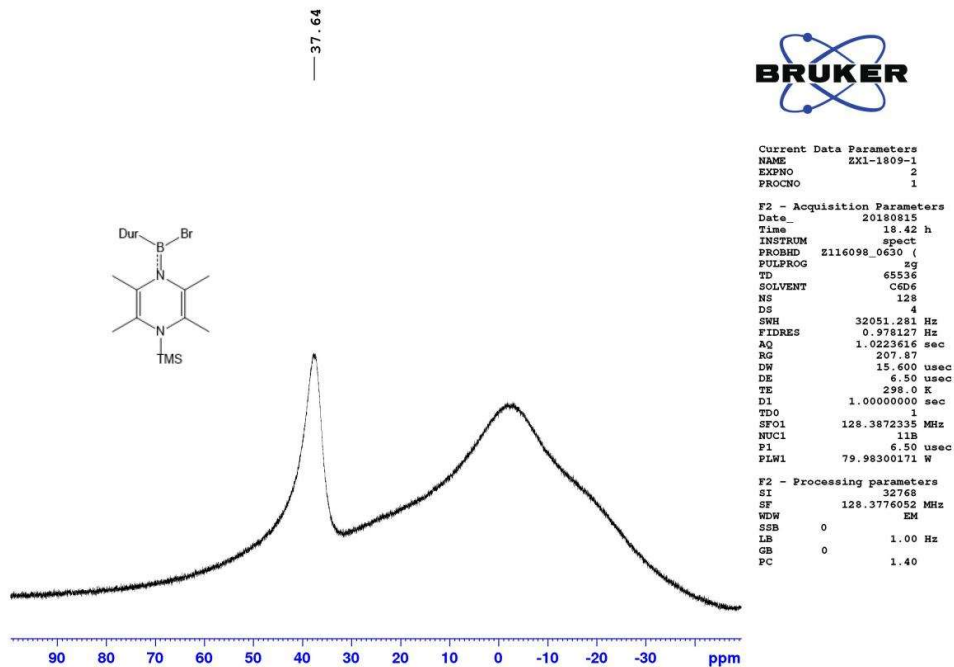


Figure S21. ^{11}B NMR (128 MHz, C_6D_6) of **9**

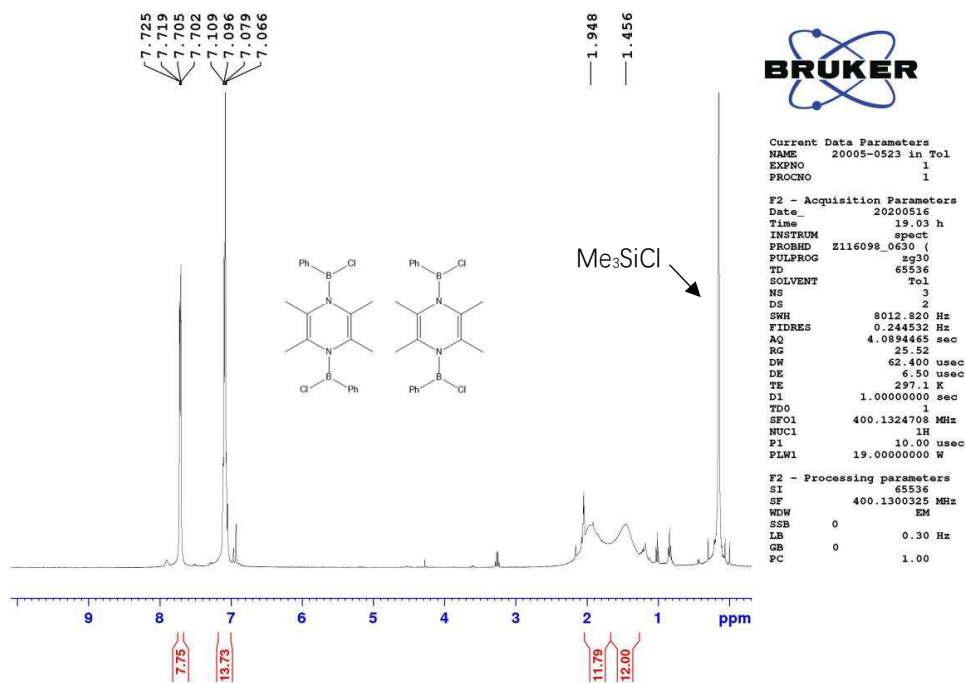


Figure S22. ^1H NMR (400 MHz, toluene- d_8) of **10a** + **10b** (Complete removal of Me_3SiCl led to partial decomposition of **10a** and **10b**)

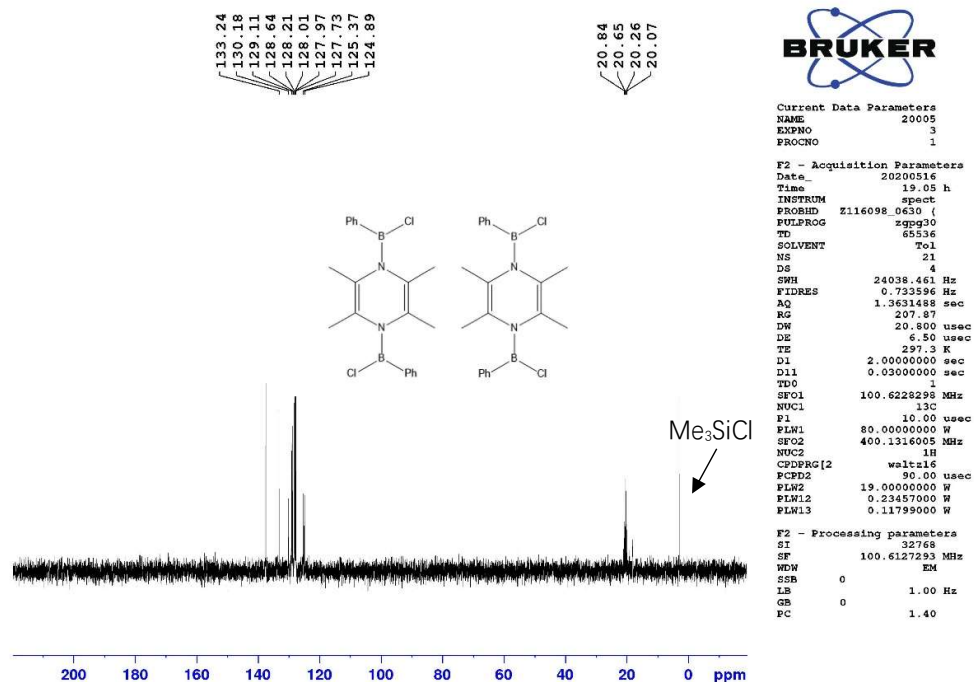


Figure S23. $^{13}\text{C}\{^1\text{H}\}$ NMR (101 MHz, toluene- d_8) of **10a** + **10b** (Complete removal of Me_3SiCl led to partial decomposition of **10a** and **10b**)

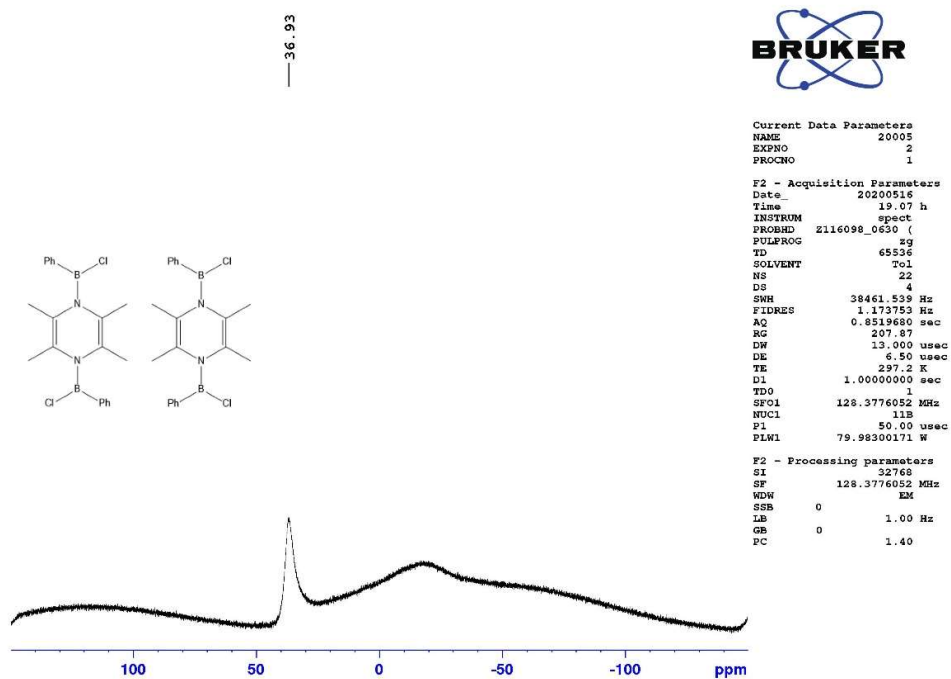


Figure S24. ^{11}B NMR (128 MHz, toluene- d_8) of **10a** + **10b**

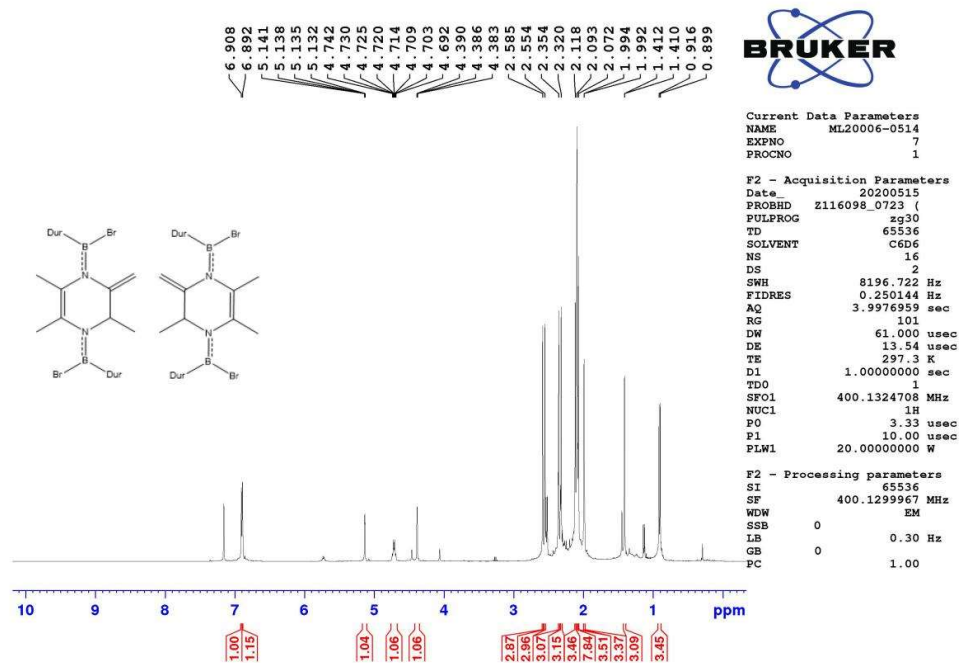


Figure S25. ^1H NMR (400 MHz, C_6D_6) of 11a + 11b

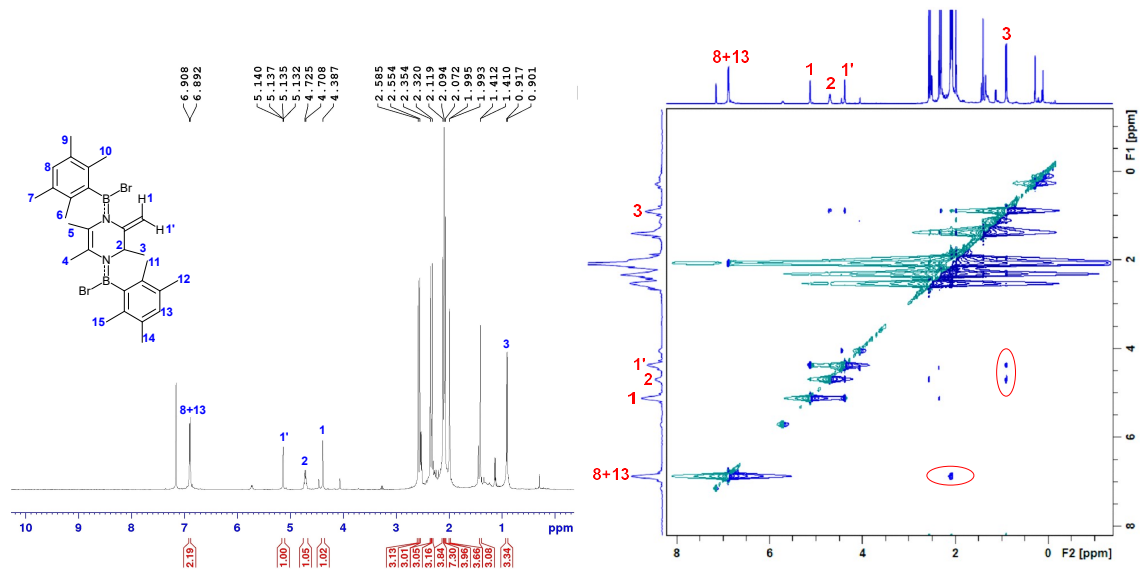


Figure S26. Assignment of 11a

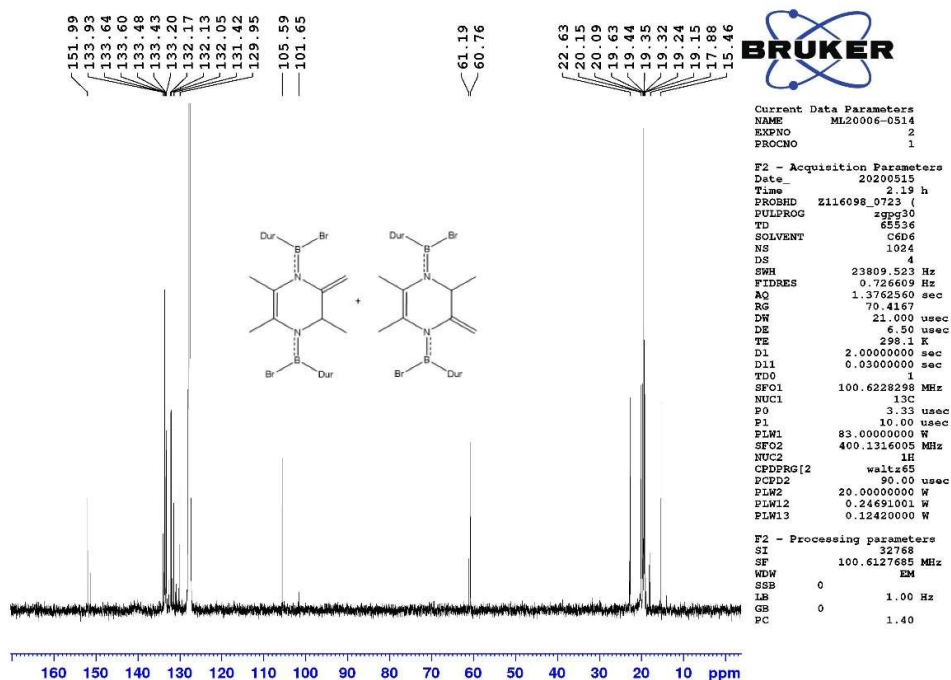


Figure S27. $^{13}\text{C}\{^1\text{H}\}$ NMR (101 MHz, C_6D_6) of 11a + 11b

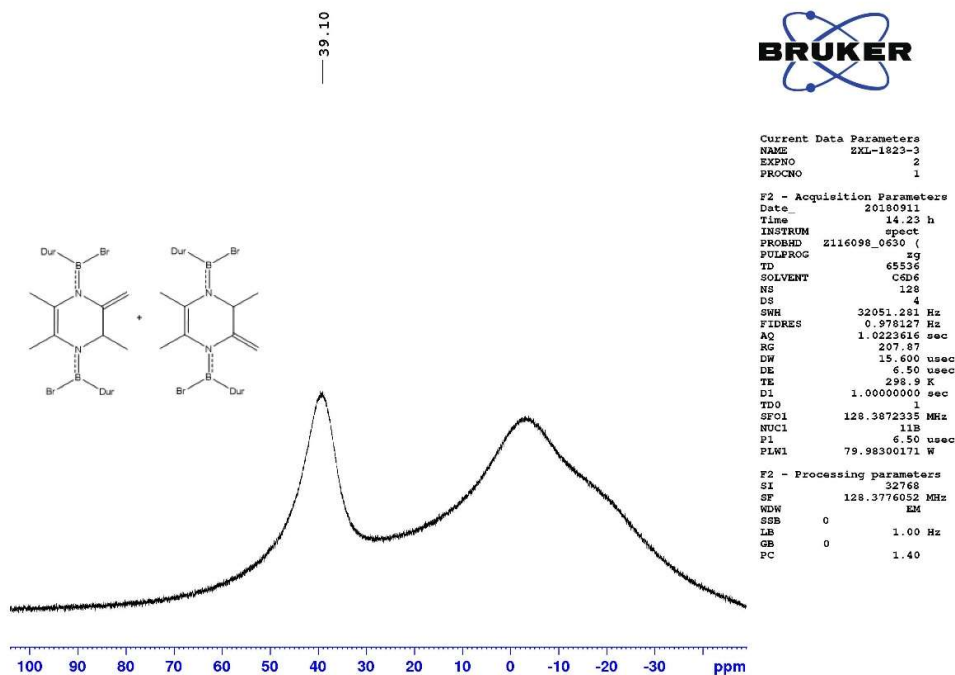


Figure S28. ^{11}B NMR (128 MHz, C_6D_6) of 11a + 11b

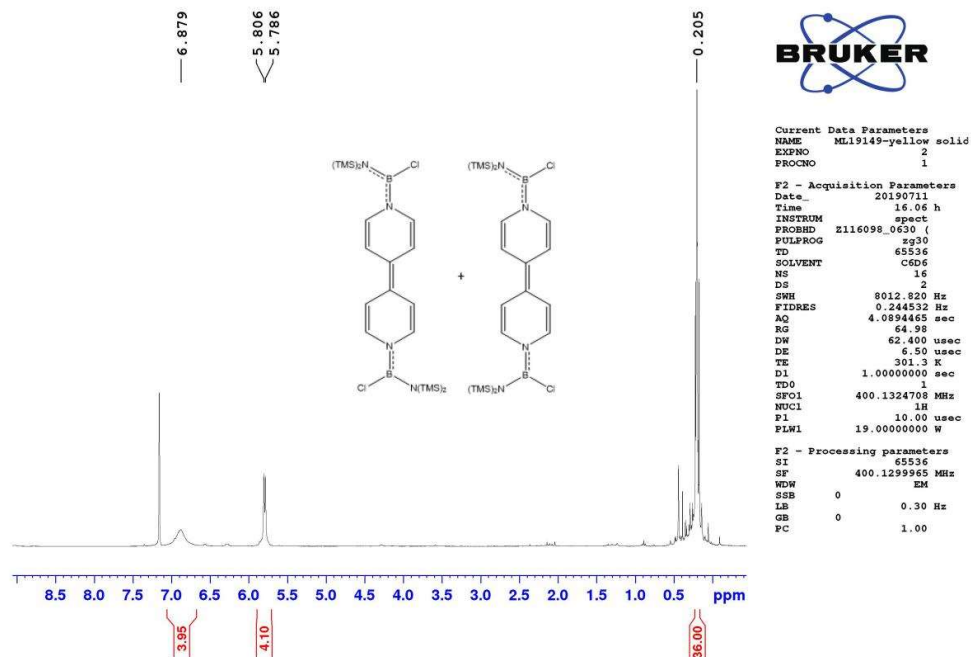


Figure S29. ^1H NMR (400 MHz, C_6D_6) of 13a + 13b

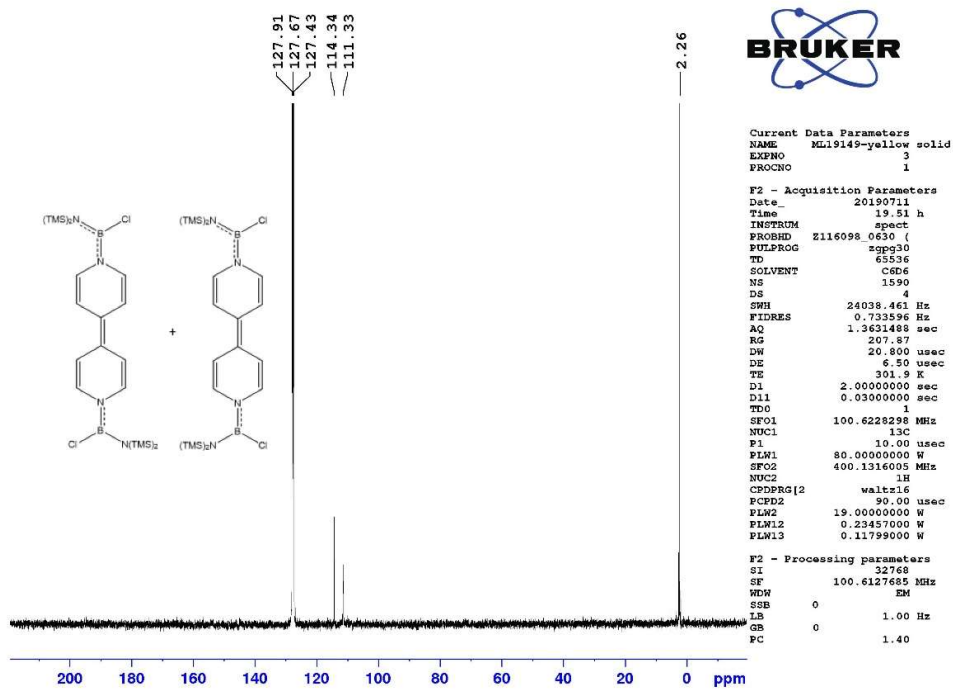


Figure S30. $^{13}\text{C}\{^1\text{H}\}$ NMR (101 MHz, C_6D_6) of 13a + 13b

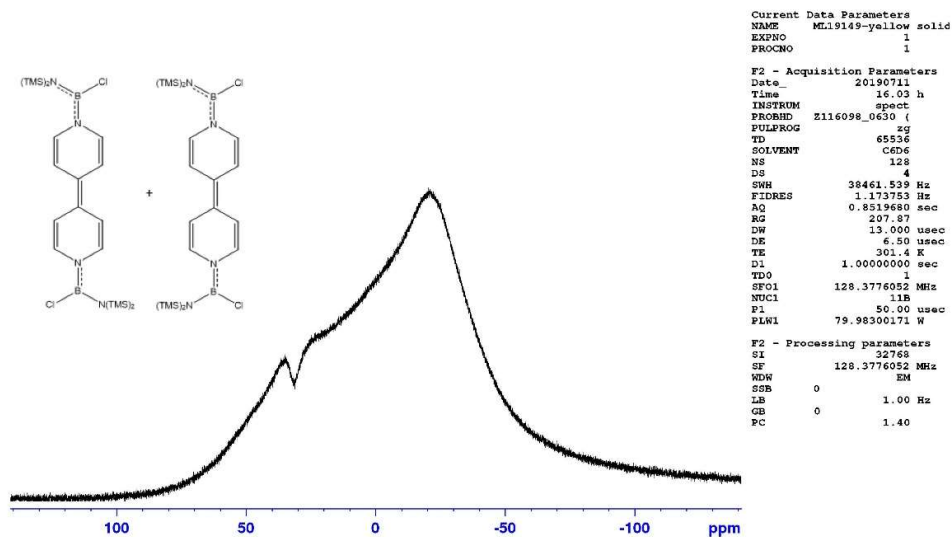


Figure S31. ¹¹B NMR (128 MHz, C₆D₆) of 13a + 13b

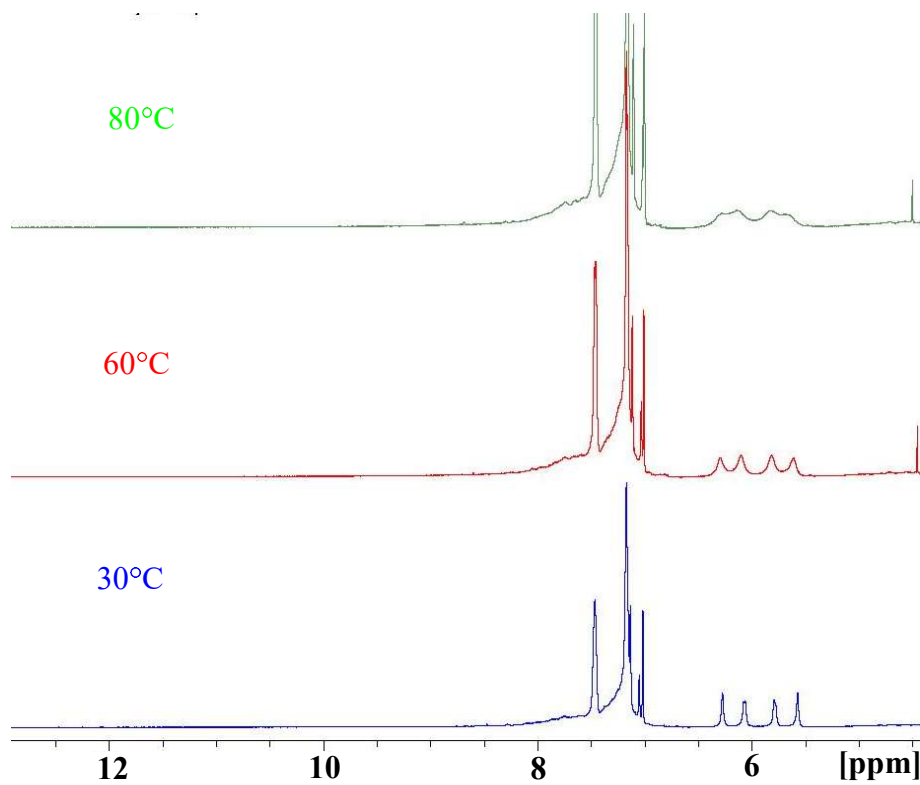


Figure S32. Variable-temperature ¹H NMR (400 MHz, toluene-d₈, 30–80 °C) of 7a + 7b

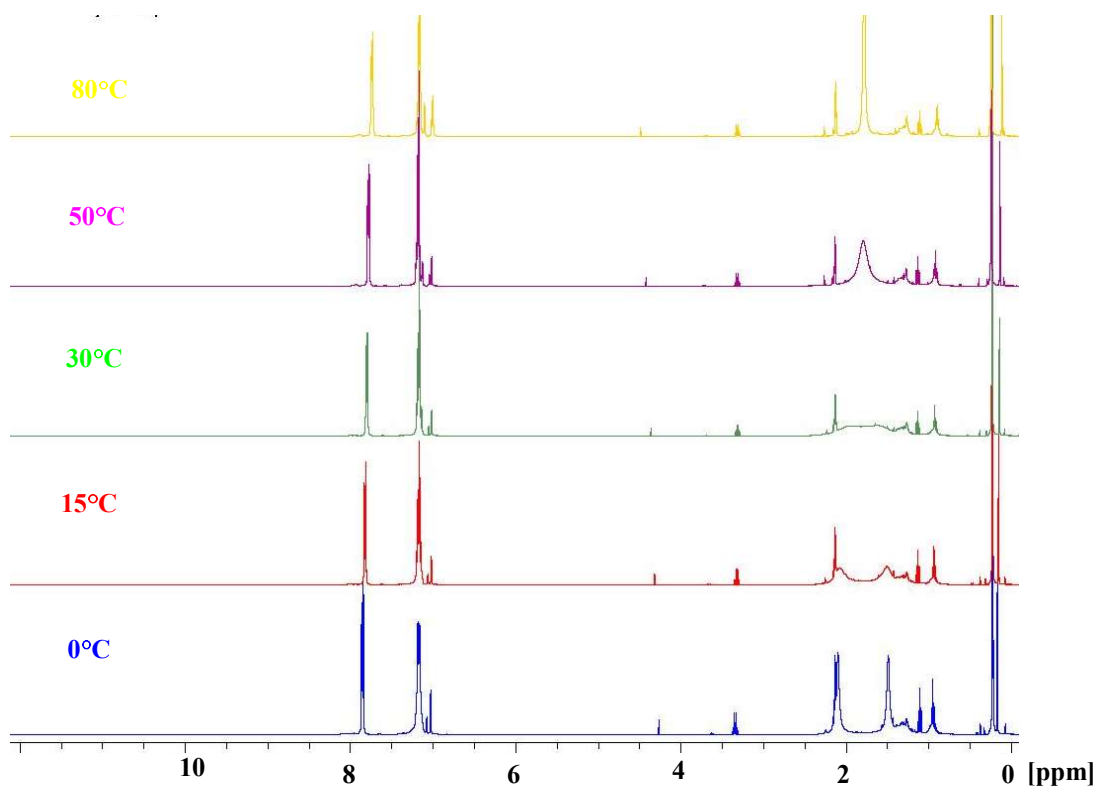


Figure S33. Variable-temperature ¹H NMR (400 MHz, toluene-d⁸, 0–80 °C) of **10a + 10b**

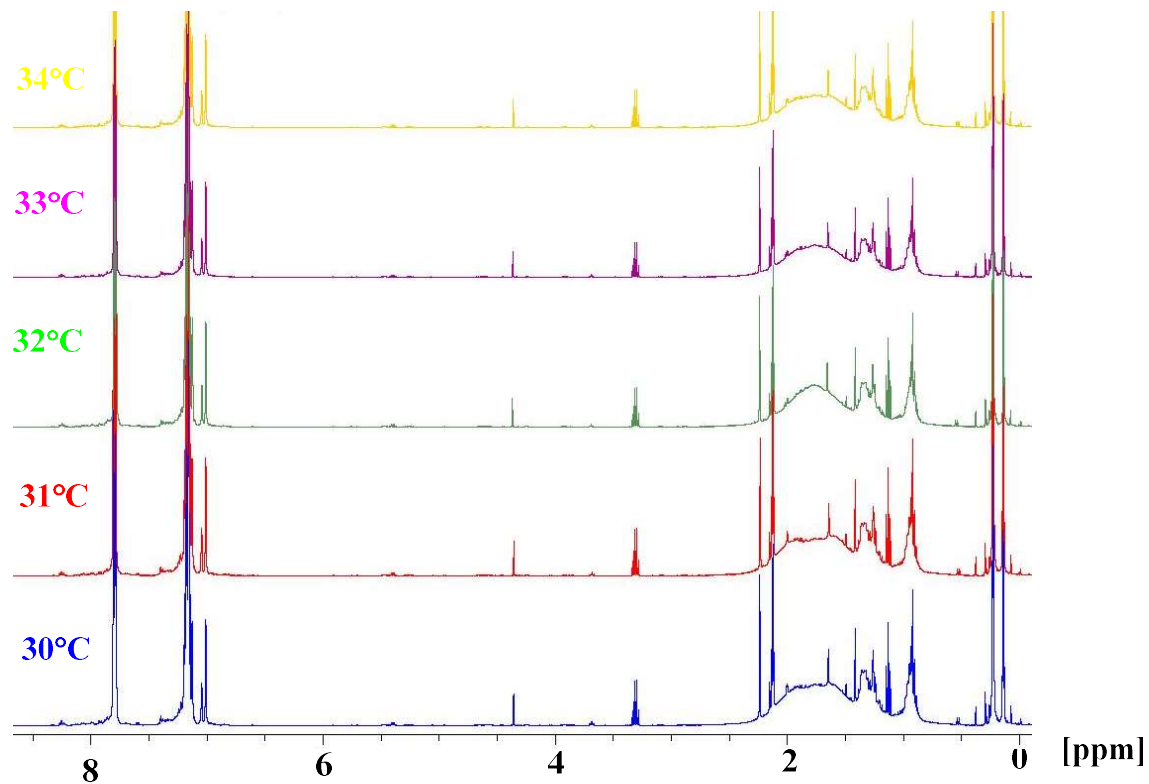


Figure S34. Variable-temperature ¹H NMR (400 MHz, toluene-d⁸, 30–35 °C) of **10a + 10b**

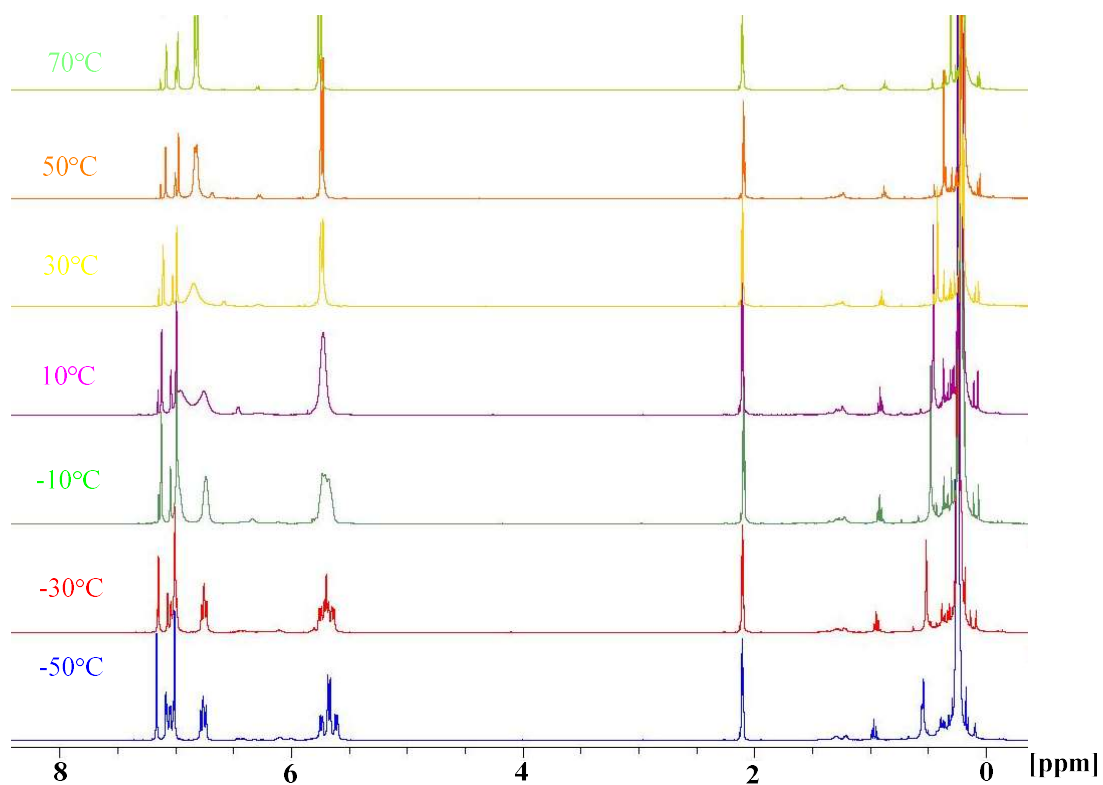


Figure S35. Variable-temperature ¹H NMR (400 MHz, toluene-d⁸, -50–70 °C) of **13a** + **13b**

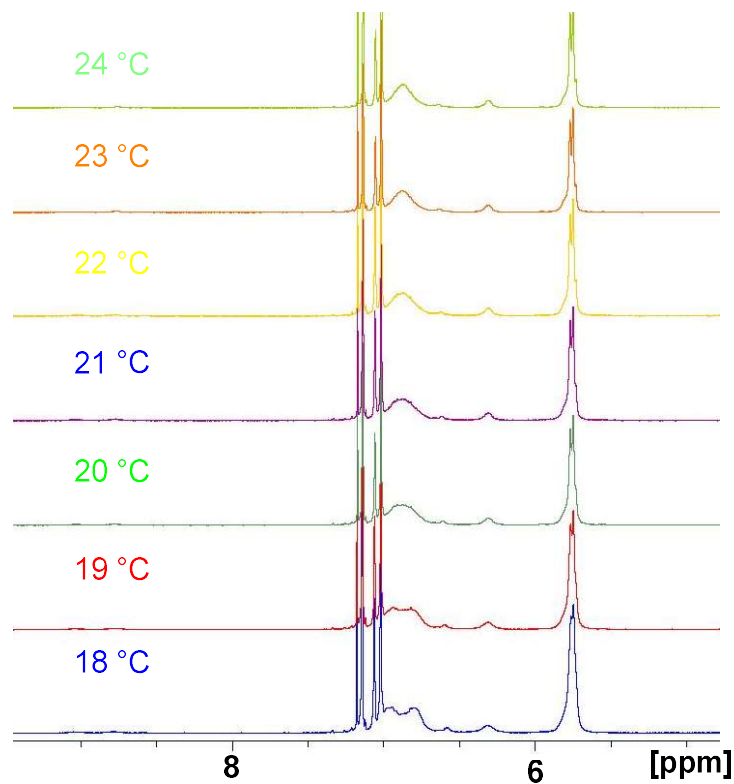


Figure S36. Variable-temperature ¹H NMR (400 MHz, toluene-d⁸, 18–24 °C) of **13a** + **13b**

II. Crystallographic details

X-ray diffraction data for compounds **5a**, **5b**, **9**, **10**, **11a**, **11b** and **13** were collected on a Bruker D8 VENTURE diffractometer with monochromated Mo-K α radiation ($\lambda = 0.71073 \text{ \AA}$). Crystals were kept at 100(2) K throughout collection. Data collection strategy determination, integration, scaling, and space group determination were performed with Apex3 software (Bruker, V2018.1-0). All structures were solved with the ShelXT structure solution program using the Intrinsic Phasing solution method^[4] and by using Olex2 as the graphical interface. The model was refined with the ShelXL program^[5] using Least Squares minimization. All non-hydrogen atoms were refined anisotropically. Hydrogen atoms were included in structure factor calculations. All hydrogen atoms were assigned to idealized geometric positions. Specific details of each experiment can be found below and in the crystallographic information files.

Crystallographic data have been deposited with the Cambridge Crystallographic Data as supplementary publication nos. CCDC-2006650 (**5**), 2006651 (**9**), 2006652 (**10**), 2006653 (**11**) and 2006654 (**13**). These data can be obtained free of charge from The Cambridge Crystallographic Data Centre *via* www.ccdc.cam.ac.uk/data_request/cif

Table S1. Crystal data for **5, 9, 10a, 11,** and **13a**

Compound	5a5b	9	10a	11a11b	13a
CCDC number	2006650	2006651	2006652	2006653	2006654
Empirical formula	C ₂₄ H ₃₀ B ₂ Br ₂ N ₂	C ₂₁ H ₃₄ BBrN ₂ Si	C ₂₀ H ₂₂ B ₂ Cl ₂ N ₂	C ₂₈ H ₃₈ B ₂ Br ₂ N ₂	C ₁₁ H ₂₂ BClN ₂ Si ₂
Formula weight	527.94	433.331	382.96	584.04	284.74
Temperature/K	100	100	100	100	100
Crystal system	monoclinic	monoclinic	monoclinic	monoclinic	monoclinic
Space group	C2/c	P2 ₁ /c	P2 ₁ /n	P2 ₁ /c	P2 ₁ /n
a/Å	21.8291(16)	18.3958(8)	9.8770(3)	11.8188(9)	6.5493(2)
b/Å	9.2690(5)	8.0538(3)	16.1316(5)	12.6999(10)	31.2087(9)
c/Å	24.5329(18)	17.2745(8)	12.8988(4)	19.1660(15)	8.4426(2)
β/°	92.665(2)	117.711(2)	92.0440(10)	96.897(3)	110.2660(10)
Volume/Å ³	4958.5(6)	2265.78(17)	2053.88(11)	2856.0(4)	1618.80(8)
Z	8	4	4	4	4
ρ _{calc} /cm ³	1.414	1.270	1.2383	1.358	1.168
μ/mm ⁻¹	3.283	1.874	0.322	2.857	0.367
F(000)	2144.0	911.8	801.4	1200.0	608.0
Crystal size/mm ³	0.02 × 0.02 × 0.006	0.4 × 0.2 × 0.2	0.4 × 0.4 × 0.2	0.06 × 0.03 × 0.03	0.123 × 0.122 × 0.111
2θ range for data collection/°	4.776 to 55.524	4.72 to 55.1	4.84 to 55.08	4.726 to 52.936	5.306 to 54.342
Reflections collected	32598	37496	16251	23838	10394
Independent reflections	5736 [R _{int} = 0.1533, R _{sigma} = 0.1140]	5208 [R _{int} = 0.0435, R _{sigma} = 0.0267]	4698 [R _{int} = 0.0362, R _{sigma} = 0.0350]	5830 [R _{int} = 0.0883, R _{sigma} = 0.0921]	3388 [R _{int} = 0.1578, R _{sigma} = 0.1614]
Data/restraints/parameters	5736/0/279	5208/0/246	4698/0/239	5830/14/340	3388/0/160
Goodness-of-fit on F ²	1.019	1.020	1.052	0.997	1.095
Final R indexes [I >= 2σ (I)]	R ₁ = 0.0669, wR ₂ = 0.1418	R ₁ = 0.0631, wR ₂ = 0.1685	R ₁ = 0.0359, wR ₂ = 0.0874	R ₁ = 0.0482, wR ₂ = 0.0936	R ₁ = 0.1345, wR ₂ = 0.3141
Final R indexes [all data]	R ₁ = 0.1333, wR ₂ = 0.1688	R ₁ = 0.0677, wR ₂ = 0.1707	R ₁ = 0.0447, wR ₂ = 0.0950	R ₁ = 0.1112, wR ₂ = 0.1117	R ₁ = 0.1889, wR ₂ = 0.3617
Largest diff. peak/hole / e Å ⁻³	0.66/-1.03	1.96/-2.31	0.36/-0.31	0.65/-0.98	1.03/-1.55

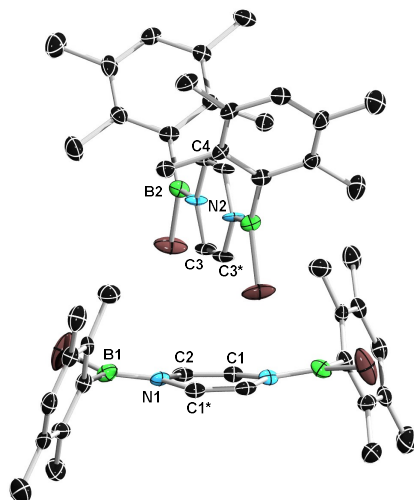


Figure S37. Single crystal structure of **5**. (Hydrogen atoms have been removed for clarity)

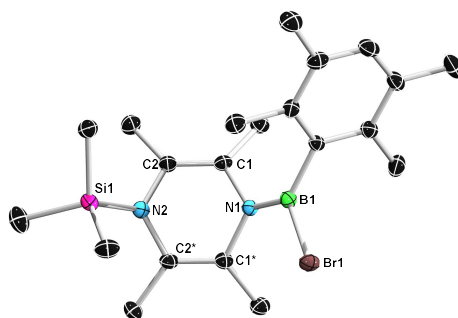


Figure 38. Single crystal structure of **9**. (Hydrogen atoms have been removed for clarity)

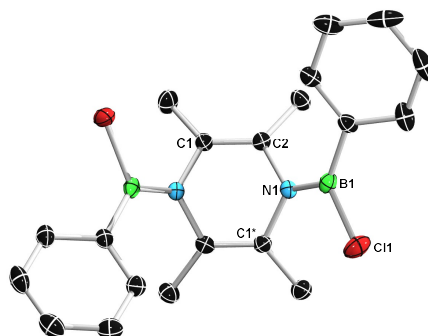


Figure S39. Single crystal structure of **10a**. (Hydrogen atoms have been removed for clarity)

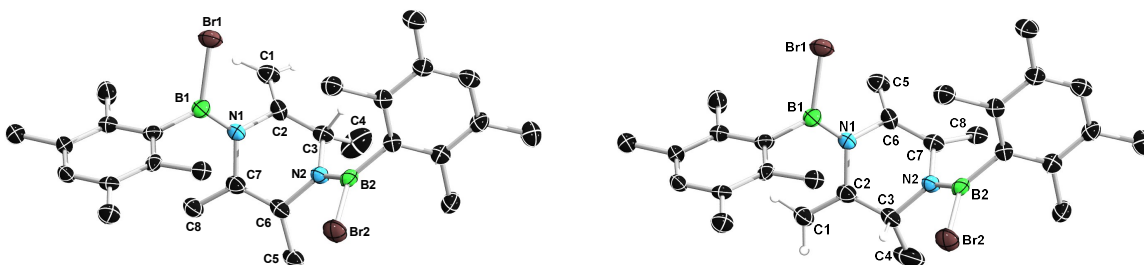


Figure S40. Single crystal structure of **11a** (left) and **11b** (right). (Hydrogen atoms have been removed for clarity)

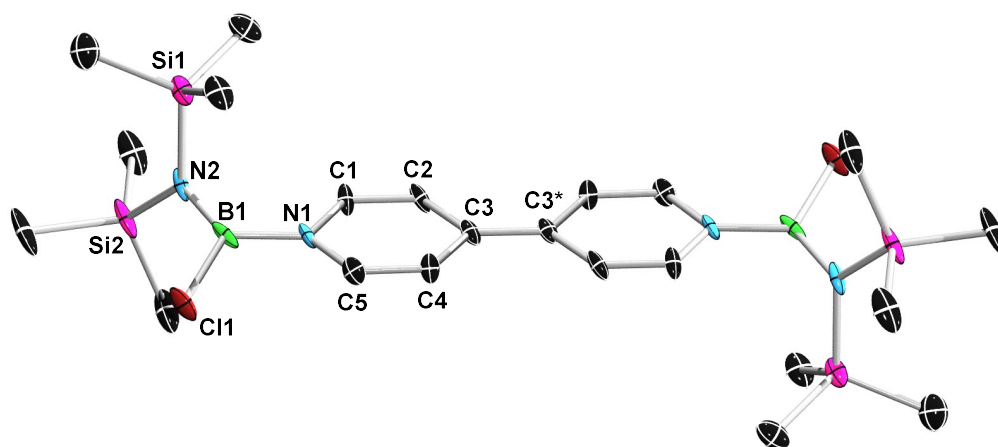


Figure S41. Single crystal structure of **13a**. (Hydrogen atoms have been removed for clarity)